C−C Bond Cleavage of Acetonitrile by a Carbonyl Iron Complex with a Silyl Ligand

Hiroshi Nakazawa,*,† Takafumi Kawasaki,‡ Katsuhiko Miyoshi,‡ Cherumuttathu H. Suresh,§ and Nobuaki Koga§

Department of Chemistry, Graduate School of Science, Osaka City University, Sugimoto, Sumiyoshi-ku, Osaka 558-8585, Japan, Department of Chemistry, Graduate School of Science, Hiroshima University, Higashi-Hiroshima 739-8526, Japan, and Graduate School of Information Science and Venture Business Laboratory, Nagoya University, Chikusa-ku, Nagoya 464-8601, Japan

Received October 4, 2002

The photoreaction of a silyl iron complex $Cp(CO)_2Fe(SiMe_3)$ (**1**) in acetonitrile in the presence of $P(NMeCH_2)_2(OMe)$ (L) yielded Cp(CO)LFeMe (**2**), CpL_2FeMe (**3**), and CpL_2Fe-(CN) (**4**), showing that carbon−carbon bond cleavage of acetonitrile was achieved. These C−C bond cleavage products were also obtained in the photoreaction of **1** with 1 equiv of MeCN in THF in the presence of L. The reaction with CD_3CN showed that the methyl group on the iron in the products is derived from acetonitrile. The corresponding reaction of $Cp(CO)_2Fe(ER_3)$ ($ER_3 = CH_3$, $GeMe_3$, $SnMe_3$) generated a CO/L exchange complex, Cp(CO)-$LFe(ER_3)$, showing that a silyl ligand on the iron is indispensable for the C−C bond cleavage of acetonitrile. Theoretical studies on the C−C bond cleavage were performed using the hybrid DFT-B3LYP method. The direct C−C bond oxidative addition of acetonitrile to the 16e species $Cp(CO)Fe(SiMe_3)$ expected to readily form from **1** in the photoreaction conditions has a very high activation barrier of 52.7 kcal/mol, suggesting that the oxidative addition is not an appropriate reaction pathway. A more feasible pathway was proposed. The end-on coordination of acetonitrile nitrogen to $Cp(CO)Fe(SiMe_3)$, followed by the rearrangement to a CN side-on complex, with the activation energy of 14.8 kcal/mol occurs, and then the insertion of the CN bond into the Fe−Si bond with a small activation energy of 4.0 kcal/mol and the successive C−C bond cleavage of acetonitrile on the Fe coordination sphere with the activation energy of 15.0 kcal/mol take place to give $Cp(CO)MeFe(CNSiMe_3)$. The isolation of an iron complex with a methyl group derived from acetonitrile and a silylisocyanide ligand was attained in the photoreaction of $Cp(CO)_2Fe(SiPh_3)$ in MeCN in the presence of PPh_3. The product Cp $(PPh_3)MeFe(CNSiPh_3)$ was confirmed by the X-ray structure analysis. The reaction mechanism leading to the iron cyanide complex has also been discussed.

Introduction

Since nitriles (R−C≡N) have relatively strong R−C and C≡N bonds and have lone pair electrons on the nitrogen atom, they have been widely used as ligands in transition metal complexes, from which they can be readily released to afford reactive and coordinatively unsaturated transition metal species. In other words, nitriles are generally resistant to the C−C bond cleavage by transition metal complexes. There are some reports exhibiting C−C bond cleavage of nitriles by transition metal complexes. They involve mainly group 10 transition metal triads[1−8] and one Mo,[9] Cu,[10] and U[11] complex. The nitrile activation has been attained by the direct oxidative addition of the C−C bond toward a transition metal center, though in many cases the mechanism has not been elucidated.

During the course of our investigation on iron phosphenium complexes,[12] we encountered C−C bond cleavage of acetonitrile promoted by an iron complex bearing a silyl ligand. Our further investigation concentrating on this C−C bond activation reaction revealed that a silyl ligand on an iron is indispensable for nitrile C−C bond cleavage, and the bond cleavage is induced by silyl migration from iron to the nitrogen in the coordinating nitrile. We here report our experimental results and

* Corresponding author. E-mail: nakazawa@sci.osaka-cu.ac.jp.
† Osaka City University.
‡ Hiroshima University.
§ Nagoya University.

(1) Burmeister, J. L.; Edwards, L. M. *J. Chem. Soc. (A)* **1971**, 1663.
(2) Gerlach, D. H.; Kane, A. R.; Parshall, G. W.; Jesson, J. P.; Muetterties, E. L. *J. Am. Chem. Soc.* **1971**, *93*, 3543.
(3) Parshall, G. W. *J. Am. Chem. Soc.* **1974**, *96*, 2360.
(4) Morvillo, A.; Truco, A. *J. Organomet. Chem.* **1981**, *208*, 103.
(5) Favero, G.; Morvillo, A.; Turco, A. *J. Organomet. Chem.* **1983**, *241*, 251.
(6) Abla, M.; Yamamoto, T. *J. Organomet. Chem.* **1997**, *532*, 267.
(7) (a) Garcia, J. J.; Jones, W. D. *Organometallics* **2000**, *19*, 5544. (b) Garcia, J. J.; Brunkan, N. M.; Jones, W. D. *J. Am. Chem. Soc.* **2002**, *124*, 9547.
(8) Miller, J. A. *Tetrahedron Lett.* **2001**, *42*, 6991.
(9) Churchill, D.; Shin, J. H.; Hascall, T.; Hahn, J. M.; Bridgewater, B. M.; Parkin, G. *Organometallics* **1999**, *18*, 2403.
(10) Marlin, D. S.; Olmstead, M. M.; Mascharak, P. K. *Angew. Chem., Int. Ed.* **2001**, *42*, 4752.
(11) Adam, R.; Villiers, C.; Ephritikhine, M.; Lance, M.; Nierlich, M.; Vigner, J. *J. Organomet. Chem.* **1993**, *445*, 99.
(12) Nakazawa, H. *J. Organomet. Chem.* **2000**, *611*, 349, and references therein.

10.1021/om0208319 CCC: $27.50
Publication on Web 12/02/2003

theoretical considerations as to acetonitrile C−C bond cleavage by an iron complex. During the preparation of this article, a quite similar paper was published by Bergman, Brookhart, and their co-workers for a rhodium complex.[13]

Results and Discussion

(a) Experimental Results. Iron silyl complex **1** was dissolved in acetonitrile and subjected to a photoreaction for 4 h in the presence of 2 equiv of diamino-substituted phosphite L (L stands for $P(NMeCH_2)_2(OMe)$ in this paper). The reaction yielded mainly three kinds of complexes (eq 1). The ^{31}P NMR spectrum of the reaction mixture showed three dominant singlets around 180 ppm in addition to a singlet at 124.51 ppm, which is attributed to free L.

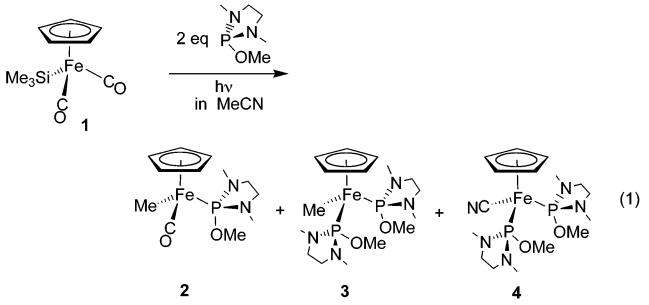

(1)

Two of the three iron complexes (**2** and **4**) could be isolated by column chromatography. The reaction mixture was loaded on an alumina column and eluted with CH_2Cl_2 to obtain a yellowish orange complex (**2**) and then eluted with acetone to obtain a yellow complex (**4**). Complex **2** was identified with Cp(CO)LFeMe, which had already been reported.[14] Complex **4** exhibits an intense IR absorption at 2063 cm^{-1} in CH_2Cl_2, indicative of a terminal CN ligand. The ^{13}C NMR spectrum, which contains a triplet at 153.6 ppm (J_{CP} = 42 Hz), also supports the existence of a CN ligand. The spectroscopic data and the single-crystal X-ray diffraction study (see below) clearly show that **4** is $CpFe(CN)L_2$. Considerable difficulty was encountered in our attempts to isolate **3** as a pure solid due to the high reactivity. Formation of **3** was evidenced by the ^1H, ^{13}C, and ^{31}P NMR measurements of the reaction mixture. The yields for the three complexes based on **1** were 15% (isolation) and 26% (from NMR) for **2**, 35% (from NMR) for **3**, and 25% (isolation) and 32% (from NMR) for **4**. Therefore, on the basis of the NMR data, 93% of complexes derived from **1** were identified after the reaction. Similar results were obtained when $Cp(CO)_2Fe(SiEt_3)$ and $Cp(CO)_2Fe(SiPh_3)$ in place of $Cp(CO)_2Fe(SiMe_3)$ were used as a starting iron complex.

These three iron-containing complexes have no silyl groups. To elucidate the fate of the $SiMe_3$ group, we examined the organic products in the reaction mixture and found the formation of Me_3SiCN and Me_4Si in 66% and 27% yields, respectively, based on **1** in eq 1.

The reaction in eq 1 obviously shows that the C−C bond of acetonitrile is cleaved by some iron complex derived from **1**. To collect more information on the unexpected reaction, we examined the following reactions. (i) The same reaction was performed by using commonly used phosphine, that is PMe_3 and PPh_3, in place of the diamino-substituted phosphite. In both cases, the corresponding products Cp(CO)(phosphine)FeMe and $Cp(phosphine)_2Fe(CN)$ were formed, whereas $Cp(phosphine)_2FeMe$ was not obtained. (ii) The reaction shown in eq 1 but in the absence of a phosphorus compound was examined, and it was found that the reaction was messy and intractable oily products were formed. The phosphorus compound added to the reaction system seems to help the isolation of methyl- and cyano-iron complexes derived from acetonitrile C−C bond cleavage (see theoretical considerations described below). (iii) To examine whether acetonitrile has to be used as a solvent, reaction of **1** with an equimolar amount of MeCN in the presence of L was conducted in THF. The results are shown in eq 2. The three iron complexes (**2**, **3**, and **4**) were formed as in eq 1, which shows that the C−C bond cleavage reaction occurred. In this case, $Cp(CO)LFe(SiMe_3)$,[14] corresponding to a CO/L exchange product of **1**, was also formed. Although the respective yields in eq 2 were slightly reduced, 65% of complexes derived from **1** were identified. (iv) When CD_3CN was

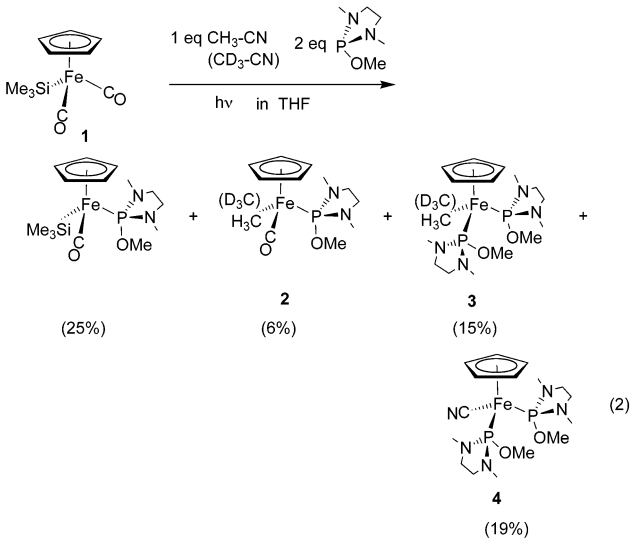

(2)

used in the reaction mentioned in (iii), $Cp(CO)LFe(CD_3)$ was obtained. This confirms that the methyl group in **2** is derived from acetonitrile but not from, for example, a $SiMe_3$ group. It is likely that $CpL_2Fe(CD_3)$ was also formed, though clear spectroscopic data could not be obtained. (v) To elucidate the role of the silyl ligand on the iron, the reactions of the corresponding alkyl, germyl, and stannyl complexes were examined (eq 3). In all cases, CO/L exchange reaction takes place to give $Cp(CO)LFe(ER_3)$.[15] Since the ^{31}P NMR spectra of the reaction mixtures showed that the yields of **8**, **9**, and **10** were more than 80%, the CO/L exchange reaction proceeds dominantly in all cases. The isolation yields were, however, 39% for **8**, 36% for **9**, and 38% for **10** presumably due to the loss of the product during the purification processes. *From these results, it can be said*

(13) Taw, F. L.; White, P. S.; Bergman, R. G.; Brookhart, M. *J. Am. Chem. Soc.* **2002**, *124*, 4192.

(14) Nakazawa, H.; Yamaguchi, Y.; Mizuta, T.; Ichimura, S.; Miyoshi, K. *Organometallics* **1995**, *14*, 4635.

(15) (a) Nakazawa, H.; Yamaguchi, Y.; Miyoshi, K. *Organometallics* **1996**, *15*, 1337. (b) Nakazawa, H.; Yamaguchi, Y.; Kawamura, K.; Miyoshi, K. *Organometallics* **1997**, *16*, 4626.

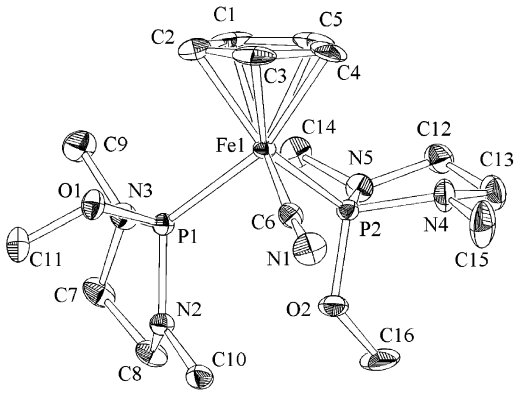

Figure 1. ORTEP drawing of **4** showing the atom-numbering scheme. The thermal ellipsoids are drawn at the 50% probability level. Hydrogen atoms are omitted for clarity.

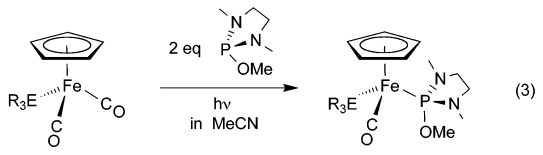

ER_3 =		
Me	**5**	**8**
$GeMe_3$	**6**	**9**
$SnMe_3$	**7**	**10**

that a silyl ligand on the iron is indispensable for the C−C bond cleavage.

The crystal structure of **4** was determined by X-ray analysis. An ORTEP drawing is displayed in Figure 1. Crystallographic data and selected bond distances and angles are summarized in Tables 1 and 2.

Complex **4** has a piano-stool configuration: the iron has a cyclopentadienyl ligand bonded in an η^5 fashion, a terminal CN ligand, and two diamino-substituted phosphite ligands. The Fe1−C6 and C6−N1 bond distances (1.907 and 1.166 Å) and the Fe1−C6−N1 angle (172.7°) are similar to those for *cis*-$[Fe(phen)_2(CN)_2]\cdot 3H_2O$, which is also an Fe(II) complex with terminal cyanide ligands.[16] The Fe−P bond distances (2.1848 and 2.1558 Å) are also similar to those for $Cp(CO)\{P(NMeCH_2)_2(OEt)\}Fe\{CH_2PPh_3\}$ (2.164 Å)[14] and $Cp(CO)\{P(NMeCH_2)_2(OEt)\}Fe\{SiMe_2PPh_3\}$ (2.1548 Å),[17] which are Fe(II) complexes with a diamino-substituted phosphite ligand.

(b) Theoretical Results. It is expected that at first the irradiation of the coordinately saturated **1** will lead to the dissociation of one of the carbonyl groups and thereby the formation of a vacant site on the Fe atom of the resulting compound $Cp(CO)Fe(SiMe_3)$, **11**. We investigated several reaction paths from **11** for the C−C bond cleavage of acetonitrile with the DFT calculations (see the Experimental Section), as shown below, to find a plausible reaction path.

The optimized structure of **11** is shown in Figure 2. One of the methyl groups of the trimethylsilyl ligand of **11** is inclined toward the vacant site on the Fe atom. This is caused by an agostic interaction[18] between the Fe atom and the methyl C−H bond, which elongates the interacting C−H bond. The C−Si bond of 1.938 Å is also longer, suggesting the agostic interaction of the C−Si bond with the iron atom.[18e]

(i) Path I: Oxidative Addition of C−C Bond. The formation of the products **2**, **3**, and **4** in eq 1 could be

Table 1. Summary of Crystal Data for 4 and 30

	4	**30**
formula	$C_{16}H_{31}Fe\,N_5O_2P_2$	$C_{43}H_{38}NPSiFe$
fw	443.25	683.69
color, habit	brown, cubic	red, cubic
cryst dimens, mm	0.25 × 0.25 × 0.15	0.20 × 0.18 × 0.07
cryst syst	monoclinic	monoclinic
unit cell dimens		
a, Å	9.1740(2)	17.643(4)
b, Å	17.7330(6)	8.135(1)
c, Å	12.5210(4)	25.519(5)
β, deg	92.412(2)	106.006(7)
V, Å^3	2035.1 (4)	3520(1)
space group	Cc(#9)	Cc(#9)
Z	4	4
D_{calcd}, g cm^{-3}	1.447	1.290
F(000)	936.00	1432.00
μ, cm^{-1}	9.18	5.39
$2\theta_{max}$, deg	55.0	55.0
no. of reflns		
measd	2471	13631
obsd($I > 3\sigma(I)$)	2354	
obsd($I > 2\sigma(I)$)		5567
struct soln	direct method (SIR92)	direct method (SIR92)
no. of params	360	424
R^a	0.027	0.067
$R_w{}^b$	0.043	0.074

^{a} $R = \sum||F_o| - |F_o||/\sum|F_o|$. ^{b} $R_w = [\sum w||F_o| - |F_c||^2/\sum w|F_o|^2]^{1/2}$ and $w = 1/\sigma^2(F_o) = [\sigma_c^2(F_o) + (p^2/4)F_\sigma{}^2]^{-1}$.

Table 2. Selected Bond Distances (Å) and Angles (deg) for 4 and 30

4		**30**	
Fe1−P1	2.1848(7)	Fe1−P1	2.182(2)
Fe1−P2	2.1558(7)	Fe1−C1	1.760(5)
Fe1−C1	2.100(3)	Fe1−C2	2.045(5)
Fe1−C2	2.087(3)	Fe1−C3	2.110(6)
Fe1−C3	2,089(3)	Fe1−C4	2.084(7)
Fe1−C4	2.086(3)	Fe1−C5	2.087(6)
Fe1−C5	2.086(3)	Fe1−C6	2.094(6)
Fe1−C6	1.907(3)	Fe1−C7	2.129(6)
P1−O1	1.635(2)	P1−C8	1.847(6)
P1−N2	1.678(2)	P1−C14	1.835(5)
P1−N3	1.682(2)	P1−C20	1.846(5)
P2−O2	1.623(2)	C1−N1	1.181(7)
P2−N4	1.686(3)	N1−Si1	1.701(6)
P2−N5	1.675(2)	Si1−C26	1.857(6)
C6−N1	1.166(4)	Si1−C32	1.862(6)
		Si1−C38	1.862(6)
P1−Fe1−P2	95.64(3)	P1−Fe1−C1	94.5(2)
P1−Fe1−C6	91.41(8)	P1−Fe1−C2	92.8(2)
P2−Fe1−C6	91.28(8)	C1−Fe1−C2	90.9(3)
Fe1−P1−O1	107.34(8)	Fe1−P1−C8	113.1(2)
Fe1−P1−N2	126.91(8)	Fe1−P1−C14	116.1(2)
Fe1−P1−N3	118.34(9)	Fe1−P1−C20	119.3(2)
Fe1−P2−O2	111.31(8)	Fe1−C1−N1	173.5(5)
Fe1−P2−N4	116.6(1)	C1−N1−Si1	156.7(5)
Fe1−P2−N5	122.49(9)	N1−Si1−C26	108.1(3)
Fe1−C6−N1	172.7(3)	N1−Si1−C32	109.4(3)
		N1−Si1−C38	107.4(3)

(16) Zhan. S.; Meng. Q.; You. X.; Wang, G.; Zheng, P.-J. *Polyhedron* **1996**, *15*, 2655.

(17) Kawamura, K.; Nakazawa, H.; Miyoshi, K. *Organometallics* **1999**, *18*, 1517.

(18) (a) Brookhart, M.; Green, M. L. H. *J. Organomet. Chem.* **1983**, *250*, 395. (b) Koga, N.; Obara, S.; Kitaura, K.; Morokuma, K. *J. Am. Chem. Soc.* **1985**, *107*, 7109. (c) Koga, N.; Obara, S.; Morokuma, K. *J. Am. Chem. Soc.* **1984**, *106*, 4625. (d) Obara, S.; Koga, N.; Morokuma, K. *J. Organomet. Chem.* **1984**, *270*, C33. (e) Koga, N.; Morokuma, K. *J. Am. Chem. Soc.* **1988**, *110*, 108. (f) Suresh, C. H.; Koga, N. *Organometallics* **2001**, *20*, 4333.

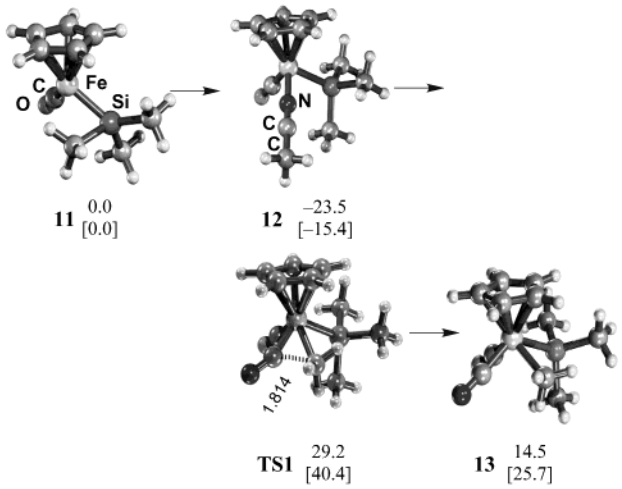

Figure 2. Path I: The oxidative addition of the CC bond of acetonitrile to Fe(II) complex. The depicted values are ZPE-corrected potential energy and the Gibbs free energy (in square brackets) in kcal/mol relative to **11** + acetonitrile.

explained by the reaction mechanism including the direct C−C bond oxidative addition of acetonitrile. However, the oxidative addition is less likely to happen. As shown in Figure 2, this reaction starts from **12** with the end-on coordination of acetonitrile to **11** and passes through the three-centered transition state **TS1** to lead to Cp(CO)MeFe(CN)($SiMe_3$), **13**. Since this reaction requires a very high activation barrier of 52.7 kcal/mol, we rule out its possibility.

(ii) Path II: C−C Bond Cleavage via the CN Bond Insertion into Fe−Si Bond. Next, let us consider the reaction from **12** described in Figure 3. The energy profile for this reaction is depicted in Figure 4 along with some bond length parameters. Complex **12** is coordinatively saturated, and without further perturbations on the electronic structure, none of the products in eq 1 (**2**, **3**, and **4**) could be formed from **12**. So we consider the transformation of **12** to the CN π-coordinated species **14**. This process takes place through **TS2** with the activation energy of 14.8 kcal/mol.

In **14**, the insertion of the CN bond into the Fe−Si bond is possible. The calculations showed that this requires only a small activation energy of 4.0 kcal/mol (cf. **TS3** in Figure 3). The Mulliken charge on silicon and nitrogen atoms of **14** was found to be 0.929 and −0.268, respectively, and therefore the silicon atom may strongly attract the negatively charged nitrogen atom toward its coordination region. The geometry of the silicon center in **TS3** is very typical of a hypervalent silicon atom[19] because the Si−C bond anti to the newly formed N−Si bond is longer compared to the other Si−C bonds by 0.03 Å (cf. Figure 4 for bond lengths). From **TS3**, a somewhat stable imino complex with the coordination of a nitrogen lone pair to the Fe atom, Cp(CO)Fe(C(Me)═$NSiMe_3$), **15**, is formed.

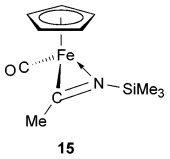

15

The main electronic change when going from **14** to **15** is the cleavage of the Fe−Si bond and the formation of the N−Si bond. The superior strength of the N−Si bond over the Fe−Si bond may account for the higher stability of **15** as compared to **14**. Note that **15** is also an Fe(II) complex with an 18-electron configuration.

If the methyl group of the imino ligand migrates to the iron atom, the methyl iron complex could be formed. We can expect such a reaction because it is similar to a decarbonylation reaction (RCO−[M] → R−[M]−CO).[20] It has been found that a distortion in **15** that breaks the Fe←N bond leads to the transition state **TS4**. This process requires an activation energy of 15.0 kcal/mol.

The Fe−N bond breaking as we go from **15** to **TS4** accounts for a decrease in the formal electron count on the iron atom by two electrons, meaning that the iron atom will formally have a vacant d orbital in **TS4**. As a result the important orbital interaction realizing the three-center transition state **TS4** arises. This is depicted in Figure 5. The methyl anion migrates to the vacant d orbital on iron, and the orbital of the CN group that was responsible for the CC bond is left as the π^* orbital. The orbital interaction depicted in Figure 5 is of great importance, as it is usually encountered in the carbonyl insertion reactions of d^8 square-planar palladium and platinum complexes.[20] The product of this step, Cp(CO)MeFe($CNSiMe_3$), **16**, is 5.9 kcal/mol more stable than **15**, which is presumably due to the presence of a strong Fe−C bond with double-bond character, viz., the Fe−C bond of length 1.796 Å (cf. Figure 4).

The reaction profile in Figure 4 well explains the rupture of the acetonitrile C−C bond by the Fe(II) complex. The highest activation barrier of 15.0 kcal/mol is well within the reach of a feasible chemical reaction. Once **16** is formed, the formation of the product **2** in eq 1 can be easily achieved by a silylisocyanide/phosphite exchange reaction. Further CO/phosphite exchange reaction on **2** would give complex **3**.

(iii) Path III: Formation of Cp(CO)MeFe(NC-$SiMe_3$) and Subsequent Reactions. While we found the reaction path for the Fe−Me bond formation, we have to look for the reaction path for the Fe−CN bond formation. At this point we come back to the Fe(II) system **16**, the Cp(CO)MeFe($CNSiMe_3$) complex (cf. Figure 3). It is expected that the dissociation of the ligand trimethylsilyl isocyanide from **16** can lead to the reaction paths for the Fe−CN bond formation. One possibility is that the dissociated trimethylsilyl isocyanide isomerizes to trimethylsilyl cyanide, of which the Si−C bond is broken by Cp(CO)MeFe, **17**. In Figures 6 and 7, the results for this reaction path are illustrated.

(19) (a) Muguruma, C.; Koga, N.; Hatanaka, Y.; El-Sayed, I.; Mikami, M.; Tanaka, M. *J. Phys. Chem. A* **2000**, *104*, 4928. (b) El-Sayed, I.; Hatanaka, Y.; Muguruma, C.; Shimada, S.; Tanaka, M.; Koga, N.; Mikami, M. *J. Am. Chem. Soc.* **1999**, *121*, 5095. (c) Weinmann, M.; Huttner, G.; Lang, H. *J. Organomet. Chem.* **1998**, *561*, 131. (d) Bearpark, M. J.; McGrady, G. S.; Prince, P. D.; Steed, J. W. *J. Am. Chem. Soc.* **2001**, *123*, 7736. (e) Perrin, L.; Maron, L.; Eisenstein, O. *Inorg. Chem.* **2002**, *41*, 4355.

(20) (a) Koga, N.; Morokuma, K. *Chem. Rev.* **1991**, *91*, 823. (b) Koga, N.; Morokuma, K. In *Quantum Chemistry: The Challenge of Transition Metals and Coordination Chemistry*; Veillard, A., Ed.; NATO ASI Series 176; : Reidel: Dordrecht, 1986; p 351. (c) Koga, N.; Morokuma, K. *J. Am. Chem. Soc.* **1985**, *107*, 7230. (d) Koga, N.; Morokuma, K. *J. Am. Chem. Soc.* **1986**, *108*, 6536. (e) Nakamura, S.; Dedieu, A. *Chem. Phys. Lett.* **1984**, *111*, 243. (f) Fukuoka, A.; Fukagawa, S.; Hirano, M.; Koga, N.; Komiya, S. *Organometallics* **2001**, *20*, 2065.

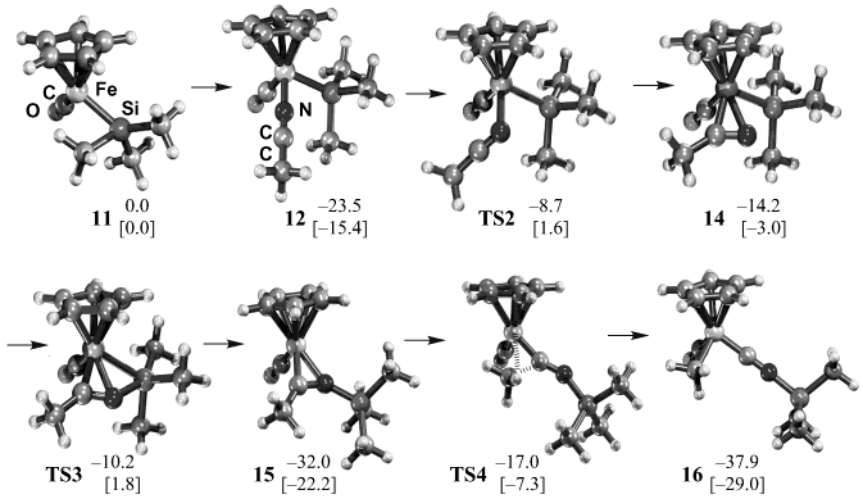

Figure 3. Path II: The cleavage of the CC bond of acetonitrile through insertion of acetonitrile into the Fe−Si bond. The depicted values are ZPE-corrected potential energy and the Gibbs free energy (in square brackets) in kcal/mol relative to **11** + acetonitrile.

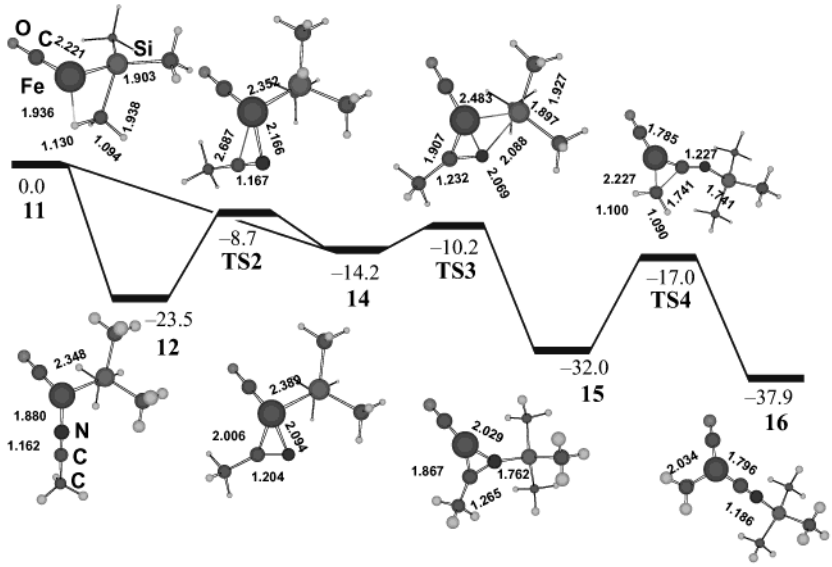

Figure 4. ZPE-corrected potential energy profile (in kcal/mol) for path II. The partial structures of the geometries (the Cp ring is excluded for clarity) are also depicted along with some bond length (in Å) parameters (the view is from the top of the Cp ring).

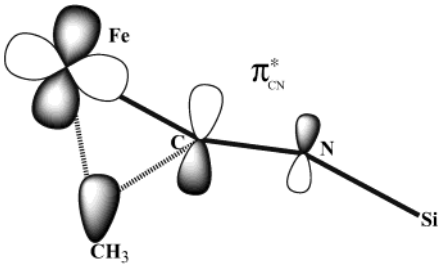

Figure 5. Three-center orbital interaction in the transition state **TS4**.

As we can see in Figure 6, the dissociation of trimethylsilyl isocyanide from **16** requires a large dissociation energy of 42.3 kcal/mol. However, such a reaction is not difficult to imagine because the unstable intermediate **17** formed in that reaction can be easily stabilized by the coordination of a solvent acetonitrile molecule. At the present level of theory, the energy of 21.3 kcal/mol is released when acetonitrile coordinates to **17**. In other words, the acetonitrile/trimethylsilyl isocyanide ligand exchange is 21.0 kcal/mol endothermic and energetically more feasible than the following isomerization of trimethylsilyl isocyanide to trimethylsilyl cyanide with the activation energy of 23.9 kcal/mol. Trimethylsilyl cyanide is more stable than trimethylsilyl isocyanide. This is in accord with the experimental fact that trimethylsilyl cyanide is thermodynamically more favorable.[21] Since the binding energy of trimethylsilyl cyanide (23.7 kcal/mol) is larger than that of acetonitrile (21.3 kcal/mol), the former would replace the latter to give trimethylsilyl cyanide complex Cp(CO)MeFe(NCSiMe_3), **18**. In fact, in the present experiments trimethylsilyl cyanide was identified in the reaction mixture (described in section (**a**)), and therefore the formation of **18** is quite likely to occur.

Complex **18** is an 18-electron Fe(II) complex in which the nitrogen of the trimethylsilyl cyanide has an end-on coordination to the iron atom, and many attempts

(21) Thayer, J. S. *Inorg. Chem.* **1968**, *7*, 2599. (b) Seckar, J. A.; Thayer, J. S. *Inorg. Chem.* **1976**, *15*, 501.

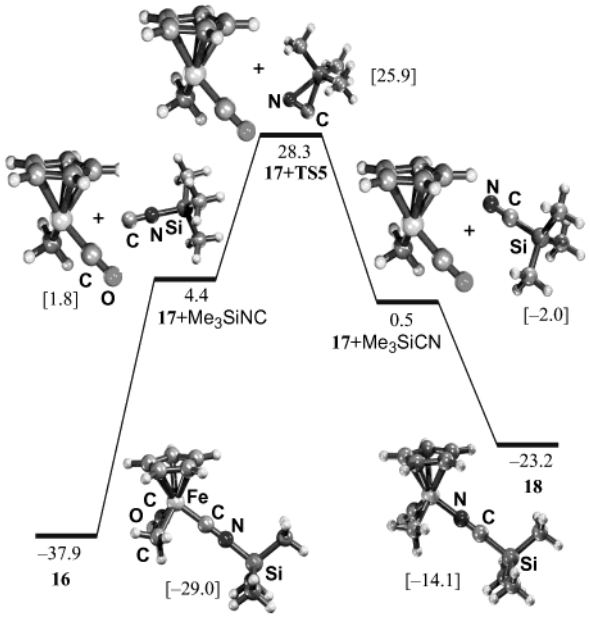

Figure 6. ZPE-corrected potential energy profile for the formation of Cp(CO)MeFe(NCSiMe$_3$), **18**, from Cp(CO)-MeFe(CNSiMe$_3$), **16**. Potential energy and the Gibbs free energy (in square brackets) relative to **11** + acetonitrile are also depicted along with the optimized geometries. All values are in kcal/mol.

to locate a transition state for the oxidative addition of the Si−CN bond of trimethylsilyl cyanide failed. Dissociation of the carbonyl group giving a coordinatively unsaturated reactive intermediate, CpMeFe(NCSiMe$_3$), **19**, is required to realize the Si−CN bond cleavage.

The breaking of the Si−CN bond starts from the side-on trimethylsilyl cyanide complex **20**. The isomerization of the end-on complex **19** to **20** passes through the transition state **TS6** with the activation energy of 15.4 kcal/mol (cf. Figures 7 and 8). Transformation of **19** to **20** weakens the Fe−N bond as it is elongated by 0.259 Å.

The Si−CN bond breaking first passes through the transition state **TS7** with the activation energy of 11.7 kcal/mol, in which the interaction of the Si−CN bond with the Fe atom makes the N atom dissociate. In the product of this step, **21**, the largely deformed trimethylsilyl cyanide seems to coordinate to iron with the help of the hypervalent character of the silicon atom.[18f] Though the Si−CN distance of 2.057 Å is only 0.165 Å longer than that of **20**, the large Fe−C−N angle of 166.0° and the short Fe−Si distance of 2.363 Å suggest that **21** is CpMeFe(CN)(SiMe$_3$) with the interaction between the Fe atom and the C−H bond as indicated by the long CH bond of 1.116 Å and the short Fe···H distance of 1.948 Å. This agostic interaction tilts the SiMe$_3$ ligand to make the silyl orbital interact with the CN π orbitals. As a matter of fact, the structure of the SiMe$_3$ ligand of **21** is similar to that of **11**.

Once the Si−CN bond is weakened in **21**, the possibility of the migration of the methyl group from iron to silicon exists.[18f] This possibility is explored in the next step, and the transition state **TS8** is located for that. Although the isomerization of **21** to CpMeFe(CN)(SiMe$_3$) with the Me and SiMe$_3$ ligands being cis to each other and their succeeding reductive elimination are expected as a possible reaction mechanism, the results show that the migration takes place in a single step without any intermediate.[22] The activation barrier is only 7.6 kcal/mol, as this transition state is quite similar to the structure of **21**. The methyl migration product **22** can be best described as the Fe(II) system with Cp(CN)Fe bound to tetramethylsilane via two Fe···H−C interactions. At this point, the formation of product **4** in eq 1 is quite easy to explain, as it corresponds to the coordination of two phosphite ligands to **22** that replaces the Fe···H−C interactions. Actually, Me$_4$Si, which is expected to be released from **22**, was experimentally detected (vide supra).

(iv) Path IV: Oxidative Addition of C−H Bond of Acetonitrile and Subsequent Reactions. There is yet another possibility that we have explored for the C−C bond cleavage of acetonitrile as well as the formation of the cyanide complex (cf. Figure 9). In this mechanism, acetonitrile approaches **11** so that one of its methyl C−H bonds interacts with the iron atom. This gives a weak complex **23**. Note that **23** is less stable than **11**+acetonitrile by 3.5 kcal/mol, indicating that the agostic interaction in **11** is stronger than the interaction between **11** and acetonitrile in **23**. The C−H···Fe interaction in **23** leads to the C−H bond oxidative addition product **24** through the transition state **TS9**. The activation energy for this step is only 6.3 kcal/mol. Note that complex **24** can be best described as a Cp(CO)-(CH$_2$CN)Fe(HSiMe$_3$) complex. If the carbonyl group dissociates from **24**, the vacant d orbital thus produced on iron will show a good interaction with the CN group of the CH$_2$CN ligand as seen in **25**. The complex **25** is also characterized by the Fe···H−Si interaction.

In the next step through the transition state **TS10**, the C−C bond of the acetonitrile fragment breaks. This step requires a moderately high activation energy of 25.0 kcal/mol. This value is not too large for the reaction to take place, because in **25** the coordination of the CN bond to Fe imposes strain on the CC bond in the FeCC triangle to activate it. The product of this step, Cp(CN)-Fe(CH$_2$)(HSiMe$_3$), **26**, is a carbene complex with Fe···H−Si interaction.

In the next step from **26**, the SiMe$_3$ group of HSiMe$_3$ migrates to the carbene ligand. This reaction passes through the transition state **TS11** to lead to Cp(CN)-Fe(H)(CH$_2$SiMe$_3$), **27**.[23] The CH$_2$SiMe$_3$ group of **27** then undergoes a minor change in its orientation with respect to the cyano group to lead to **TS12**. Then the hydrogen atom migrates to the carbon atom of the CH$_2$SiMe$_3$ fragment, so that finally Cp(CN)Fe(H$_3$CSiMe$_3$), **28**, is given. The structure of complex **28** has two Fe···CH interactions similar to that of complex **22** in path III. The main difference between **28** and **22** is that in the former the Fe···CH interactions are from the same methyl group, while in the latter such interactions are from different methyl groups. The formation of the product **4** in eq 1 is achieved when H$_3$CSiMe$_3$ in **28** is replaced with the phosphites.

(22) In the model reaction with SiH$_3$ in place of SiMe$_3$, there is CpMeFe(CN)(SiH$_3$) with the Me and SiH$_3$ groups being cis to each other as an intermediate.

(23) Instead of the SiMe$_3$ group, the hydrogen atom of the newly formed Fe−H bond of **26** can also migrate back to the carbene ligand. The activation energy needed for this was the same as that for the **26** to **27** conversion. However, the reaction profile consisting of the hydrogen migration product that leads to the agostic complex **28** was placed at higher energy level than that described in the reaction profile depicted in Figure 9. So we do not describe this path in detail.

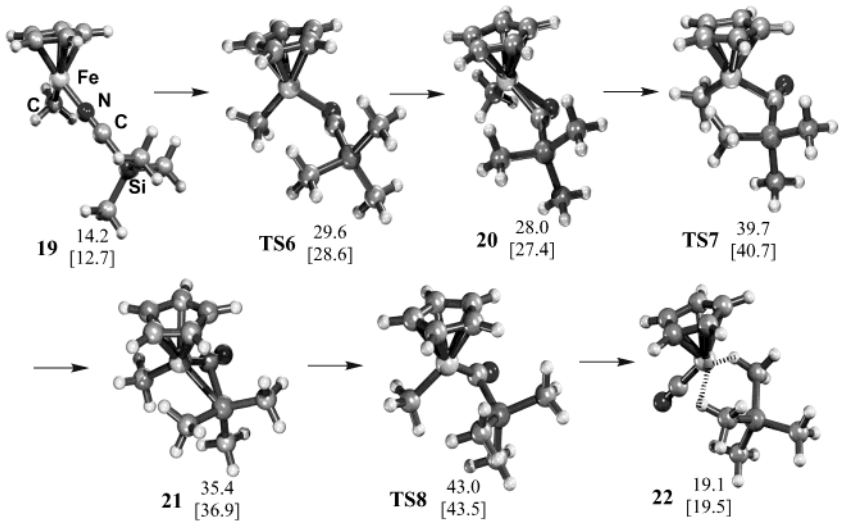

Figure 7. Path III: The cleavage of the Si−CN bond of trimethylsilyl cyanide activated by Fe(II) complex. ZPE-corrected potential energy and the Gibbs free energy (in square brackets) in kcal/mol relative to **11** + acetonitrile are depicted.

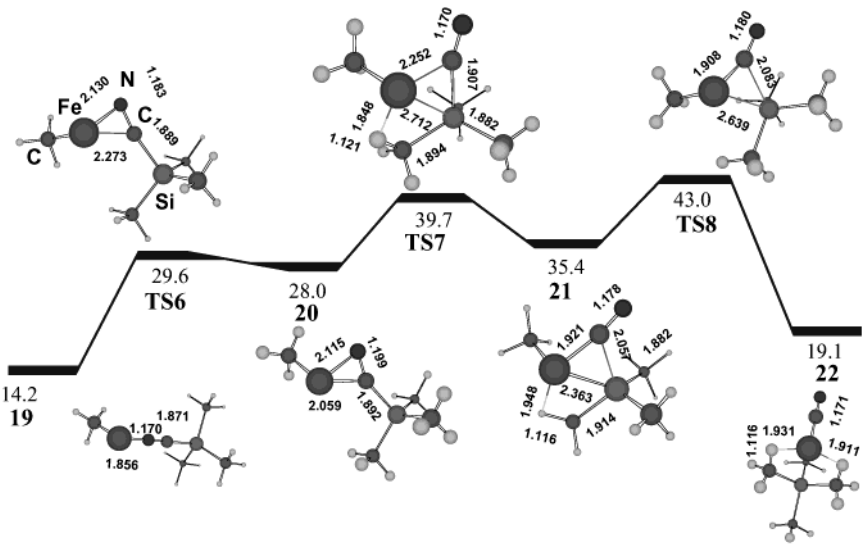

Figure 8. ZPE-corrected potential energy profile (in kcal/mol) for path III. The partial structures of the geometries (Cp ring is excluded) are also depicted along with some bond length (in Å) parameters (the view is from the top of the Cp ring).

As we can see, the reaction path IV described above and path III (cf. Figures 6, 7, and 8) can give the cyanide complex **4** in eq 1. However, path III is the most preferred one, as it needs the highest activation energy of 23.9 kcal/mol as compared to that of 25.0 kcal/mol required for the CC bond cleavage step of path IV (cf. Figure 9). Further, path IV is thermodynamically less favorable than path III, as it contains intermediates and transition states with very high energies. Moreover, during the reaction path IV, $HSiMe_3$ dissociation is possible. For instance, that from **25** is endothermic by only 8.0 kcal/mol, indicating that $HSiMe_3$ dissociation is easier than CC bond cleavage and that the cyanomethyl complex should be detected.

(v) Path V: Me_3Si Migration in the Me_3SiNC Complex. Another possibility for the Fe−CN bond formation is via the Me_3Si migration to the iron atom in Cp(CO)MeFe(CNSiMe_3), **16**. However, this reaction can be neglected because the DFT calculations showed that this process required a large activation energy of 51.3 kcal/mol. The CO dissociation from **16** reduces the activation energy to 37.2 kcal/mol, but it is still too large.

(c) Further Experiments that Validate Theoretical Results. In the theoretical considerations, it is assumed that at first a carbonyl ligand is liberated from **1** by photolysis to give the 16e species Cp(CO)Fe($SiMe_3$). This was supported by the experimental fact that Cp(CO)LFe($SiMe_3$) was detected in the reaction of **1** with an equimolar amount of MeCN in the presence of L in THF. We have also seen that the theoretical consideration as to the C−C bond cleavage by the iron silyl complex proposed that silyl migration from iron to the nitrogen in coordination nitrile takes place to give an iron complex having methyl and silylisocyanide ligands (complex **16** in Figure 3). In fact, the detection of the compound Me_3SiCN as described in section (**a**) strongly supported the formation of **16** as well as the whole mechanism given in Figure 4 (path II). It is felt that the detection of complex **16** itself will further confirm the mechanism.

Therefore, to isolate complex **16**, several attempts were made, and it was finally found that a photoreaction of $Cp(CO)_2Fe(SiPh_3)$ (**29**) in the presence of PPh_3 in acetonitrile yielded Cp(PPh_3)MeFe(CNSiPh_3) (**30**) (eq 4).

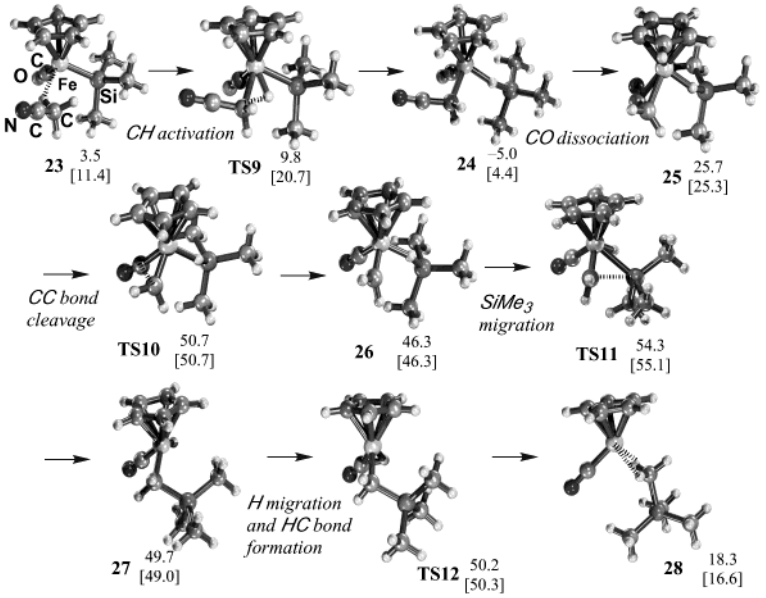

Figure 9. Path IV: Oxidative addition of the C−H bond of acetonitrile and subsequent reactions. The depicted values are ZPE-corrected potential energy and the Gibbs free energy (in square brackets) in kcal/mol relative to **11** + acetonitrile.

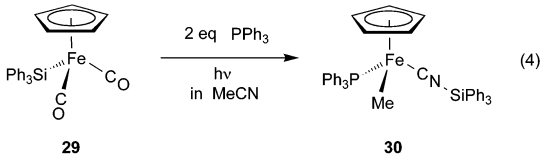

Complex **30** was isolated as red crystals. The ^{31}P NMR spectrum showed a signal at 87.60 ppm, which was assigned to coordinating PPh_3. In the ^{13}C NMR spectrum, there were two characteristic resonances: a doublet at −21.07 ppm with $J = 23.5$ Hz due to a methyl ligand and a doublet at 221.23 ppm with $J = 35.5$ Hz due to a silylisocyanide ligand. The complex exhibited an intense IR absorption at 1926 cm^{-1} attributable to CN stretching. These spectroscopic data suggest that the isolated complex **30** is formulated as $Cp(PPh_3)MeFe(CNSiPh_3)$.

The structure was confirmed by X-ray analysis, which is depicted in Figure 10. It clearly shows that C−CN bond cleavage took place. The C−N bond distance (1.181 Å) is longer than that for $[Cp^*(PMe_3)(^iPr)Rh(CNSiPh_3)]^+$,[13] indicating that π-back-donation from the iron fragment to the π^* orbital of the CN multiple bond is stronger than that from the Rh fragment. This is reasonably understood from the cationic Rh fragment. It is noteworthy that the C−N bond distance for **30** is longer than that for **4** (1.166 Å). Since both are electronically neutral Fe(II) complexes, it shows that the $CNSiPh_3$ ligand is a better π-acceptor than the CN ligand. The C−N−Si angle for **30** is 156.7°, whereas that for $[Cp^*(PMe_3)(^iPr)Rh(CNSiPh_3)]^+$ is 175.9° (cf. Tables 1 and 2). The angle for **30** seems to be due to steric repulsion between the bulky PPh_3 and $SiPh_3$ groups.

Conclusions

The reactions mentioned above are quite rare examples of the activation of a C−C bond connected to a cyanide group promoted by a transition metal complex with a silyl ligand.[13] The experimental results and the DFT level calculations starting from $[Cp(CO)Fe(SiMe_3)]$ (**11**) proposed that the mechanism of the C−C bond cleavage corresponds to the insertion of CN of acetonitrile to the Fe−Si bond, followed by methyl migration to iron to give complex **16**. The reaction sequences are depicted with line drawings in Figure 11. The CN insertion and the methyl migration required activation energies of 14.8 and 15.0 kcal/mol, respectively. The low

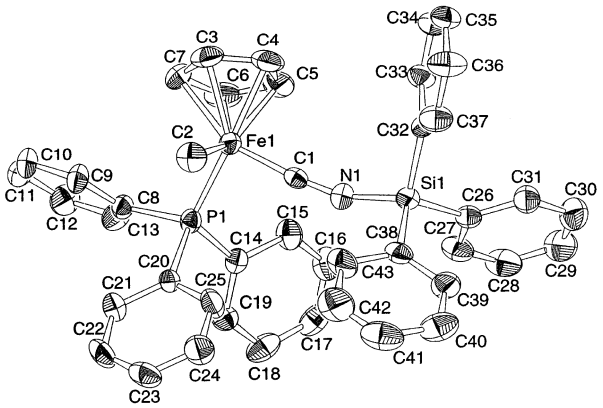

Figure 10. ORTEP drawing of **30** showing the atom-numbering scheme. The thermal ellipsoids are drawn at the 50% probability level. Hydrogen atoms are omitted for clarity.

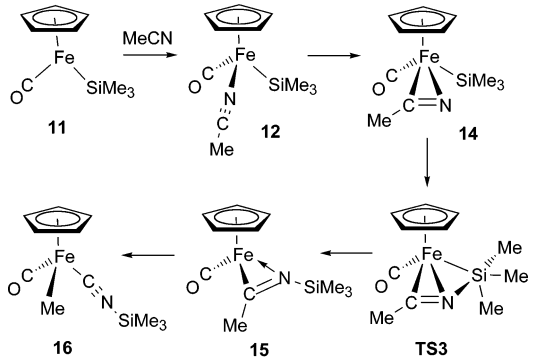

Figure 11. Reaction sequences of acetonitrile CC bond cleavage depicted with line drawings.

activation barrier for the CN insertion reaction is attributed to the hypervalent character of the silicon atom and the charge distribution of the nitrogen and silicon atoms. Both experiment and theory supported the formation of Me_3SiCN in the reaction mixture. The formation of Fe(II) cyanide complex (**4**) is due to the reaction that led to the cleavage of the Si−CN bond of Me_3SiCN in the coordination sphere of the CpMe(CO)-Fe complex. In the formation of complexes **2**, **3**, and **4**, the hypervalent character of the silicon atom played a major role.

Experimental Section

General Remarks. All reactions were carried out under an atmosphere of dry nitrogen using standard Schlenk techniques. Column chromatography was done quickly in the air. MeCN, CH_2Cl_2, and THF were distilled from CaH_2, P_2O_5, and sodium metal, respectively, and then they were stored under a dry nitrogen atmosphere. P{$NMeCH_2$}$_2$(OMe),[24] $Cp(CO)_2Fe(SiMe_3)$,[25] and $Cp(CO)_2Fe(SiPh_3)$[26] were prepared according to the literature method.

IR spectra were recorded on a Shimadzu FTIR-8100A or a Perkin-Elmer Spectrum One spectrometer. A JEOL LA-300 multinuclear spectrometer was used to obtain ^{1}H, ^{2}D, ^{13}C, and ^{31}P NMR spectra. ^{1}H and ^{13}C NMR data were referenced to Me_4Si, and ^{31}P NMR data were referenced to 85% H_3PO_4. The chemical shift in ^{2}D NMR was referred to the resonance of $CDCl_3$ at 7.24 ppm. Elemental analysis data were obtained on a Perkin-Elmer 2400 CHN elemental analyzer.

Photoreaction of 1 in MeCN in the Presence of P(NMeCH$_2$)$_2$(OMe). $Cp(CO)_2Fe(SiMe_3)$ (3.4 mmol), MeCN (70 mL), and P($NMeCH_2$)$_2$(OMe) (6.8 mmol) were put in a Pyrex Schlenk tube, and the solution was irradiated with a 400 W medium-pressure mercury arc lamp at 0 °C for 4 h. After the solvent was removed, the residue was loaded on an alumina column. An orange complex eluted with CH_2Cl_2 and a yellow complex eluted with acetone were collected respectively and dried in vacuo to give yellow powders of **2** and **4**. The isolation yields were 15% for **2** and 25% for **4** based on **1**. The spectroscopic data for **2** were identical to those for Cp(CO)-{P($NMeCH_2$)$_2$(OMe)}FeMe, which has already been reported.[14]

4: IR (ν_{CN}, in CH_2Cl_2): 2063. ^{1}H NMR (δ, in $CDCl_3$): 2.70 (d, $^3J_{PH}$ = 4.8 Hz, 3H, NCH_3), 2.72 (d, $^3J_{PH}$ = 5.1 Hz, 3H, NCH_3), 2.82 (d, $^3J_{PH}$ = 4.8 Hz, 3H, NCH_3), 2.84 (d, $^3J_{PH}$ = 5.1 Hz, 3H, NCH_3), 3.00−3.05 (m, 4H, NCH_2), 3.14−3.30 (m, 4H, NCH_2), 3.20 (d, $^3J_{PH}$ = 5.3 Hz, 3H, OCH_3), 3.21 (d, $^3J_{PH}$ = 5.5 Hz, 3H, OCH_3), 4.28 (s, 5H, C_5H_5). ^{13}C NMR (δ, in $CDCl_3$): 33.73 (m, NCH_3), 51.22 (d, $^2J_{PC}$ = 6.2 Hz, OCH_3), 51.30 (d, $^2J_{PC}$ = 6.2 Hz, OCH_3), 51.47 (s, NCH_2), 51.73 (s, NCH_2), 78.74 (s, C_5H_5), 153.58 (t, $^2J_{CP}$ = 41.9 Hz, CN). ^{31}P NMR (δ, in CH_2Cl_2): 174.72. Anal. Calcd for $C_{16}H_{31}FeN_5O_2P_2$: C, 43.36; H, 7.05; N, 15.80. Found: C, 43.54; H, 7.12; N, 15.80.

Formation of **3** was evidenced by the ^{1}H, ^{13}C, and ^{31}P NMR measurements of the reaction mixture mentioned above, together with those of the reaction mixture containing mainly **2** and **3** in the photoreaction of [$Cp(CO)_2FeMe$] with L in acetonitrile.

3: ^{1}H NMR (δ, in $CDCl_3$): −0.59 (t, $^3J_{PH}$ = 6.0 Hz, 3H, $FeCH_3$), 4.11 (s, 5H, C_5H_5). ^{13}C NMR (δ, in $CDCl_3$): −27.77 (t, $^2J_{PC}$ = 34.4 Hz, $FeCH_3$), 79.13 (s, C_5H_5). ^{31}P NMR (δ, in $CDCl_3$): 180.25 (s).

Formation of $Cp(CO)LFe(CD_3)$ (**2**-CD_3) was evidenced by the ^{1}H, ^{2}D, ^{13}C, and ^{31}P NMR measurements of the reaction mixture, together with those of the reaction mixture produced in the photoreaction of **1** with 1 equiv of CD_3CN in the presence of L in THF.

2-CD$_3$: ^{1}H NMR (δ, in $CDCl_3$): 4.37 (s, 5H, C_5H_5). ^{2}D NMR (δ, in $CHCl_3$): −0.23 (s, CD_3). ^{13}C NMR (δ, in $CDCl_3$): −26.33 (d of sept, $^2J_{PC}$ = 30.4 Hz, $^1J_{DC}$ = 20.3 Hz, $FeCD_3$), 82.56 (d, $^2J_{PC}$ = 1.2 Hz, C_5H_5), 222.48 (d, $^2J_{PC}$ = 46.6 Hz, CO). ^{31}P NMR (δ, in $CDCl_3$): 177.68 (s).

Photoreaction of 5, 6, or 7 in MeCN in the Presence of P(NMeCH$_2$)$_2$(OMe). $Cp(CO)_2FeMe$ (3.4 mmol), MeCN (70 mL), and P($NMeCH_2$)$_2$(OMe) (6.8 mmol) were put in a Pyrex Schlenk tube, and the solution was irradiated with a 400 W medium-pressure mercury arc lamp at 0 °C for 4 h. After the solvent was removed, the residue was loaded on an alumina column. A yellow complex eluted with hexane was collected and dried in vacuo to give yellow powders of **8**.[14] The isolation yield based on $Cp(CO)_2FeMe$ was 39%. The reactions of **6** and **7** were undertaken similarly to give **9** (isolation yield, 36%) and **10** (isolation yield, 38%), respectively.

Preparation of 30. $Cp(CO)_2Fe(SiPh_3)$ (0.77 g, 1.76 mmol), PPh_3 (0.93 g, 3.55 mmol), and MeCN (20 mL) were put in a Pyrex Schlenk tube, and the solution was irradiated with a 400 W medium-pressure mercury arc lamp at 0 °C for 4 h. An orange powder thus formed was washed with MeCN (5 mL × 4) and dried in vacuo. The powder was dissolved in toluene (3 mL), and the solution was charged on a Celite column. An orange band eluted with toluene was collected, and the solvent was removed under reduced pressure to give **30** as an orange powder (0.39 g, 0.57 mmol, yield 33%). IR (ν_{CN}, in CH_2Cl_2): 1926. ^{1}H NMR (δ, in $CDCl_3$): −0.22 (d, $^3J_{PH}$ = 6.6 Hz, 3H, $FeCH_3$), 4.08 (s, 5H, C_5H_5), 7.06−7.49 (m, 30H, Ph). ^{13}C NMR (δ, in $CDCl_3$): −21.07 (d, $^2J_{PC}$ = 23.5 Hz, $FeCH_3$), 83.94 (s, C_5H_5), 127.54 (d, J_{CP} = 8.7 Hz, PPh_3), 127.92 (s, $SiPh_3$), 128.69 (d, J_{CP} = 1.9 Hz, PPh_3), 130.08 (s, $SiPh_3$), 133.32 (d, J_{CP} = 10.0 Hz, PPh_3), 133.34 (s, $SiPh_3$), 135.04 (s, $SiPh_3$), 137.96 (d, J_{CP} = 36.6 Hz, PPh_3), 221.23 (d, $^2J_{CP}$ = 35.5 Hz, FeCN). ^{31}P NMR (δ, in $CDCl_3$): 87.60. Anal. Calcd for $C_{43}H_{38}FeNPSi$: C, 75.54; H, 5.60; N, 2.05. Found: C, 75.75; H, 5.62; N, 1.55.

X-ray Structure Determination for 4 and 30. Suitable crystals of **4** and **30** were obtained through crystallization from toluene/hexane and from CH_2Cl_2/hexane, respectively, and were mounted individually on a glass fiber. All measurements for **4** and **30** were made on a Mac Science DIP2030 diffractometer and on a Rigaku/MSC Mercury CCD diffractometer, respectively, with graphite-monochromated Mo Kα radiation (λ = 0.710 73 Å) at 200 K. Crystal data, data collection parameters, and results of the analysis are summarized in Table 1.

The structures were solved by direct methods with the program SIR92[27] and expanded using Fourier techniques.[28] Positions of hydrogen atoms were determined from subsequent difference Fourier maps. The non-hydrogen atoms were refined anisotropically. Hydrogen atoms were refined isotropically. An extinction correction was applied. All calculations were performed using the program package teXsan.[29]

Details of Computational Method. All the molecular geometries were optimized at the DFT level of theory using the B3LYP hybrid functional[30] with the Gaussian 98 suite of programs.[31] For Fe, the basis set LanL2DZ was used.[32] In this basis set the 10 innermost electrons of Fe have been replaced by an effective core potential (ECP) of Hay and Wadt.[32] For H, C, N, O, and Si, 6-31G(d) basis functions were selected.[33]

(24) Ramirez, F.; Paatwardham, A. V.; Kugler, H. J.; Smith, C. P. *J. Am. Chem. Soc.* **1967**, *89*, 6272.
(25) King, R. B.; Pannel, K. H. *Inorg. Chem.* **1968**, *7*, 1500.
(26) Cerveau, G.; Colomer, E.; Corriu, R.; Douglas, W. E. *J. Organomet. Chem.* **1977**, *135*, 373.
(27) Aotomare, A.; Burla, M. C.; Camalli, M.; Cascarano, M.; Giacovazzo, C.; Gaugliardi, A.; Polidori, G. *J. Appl. Crystallogr.* **1994**, *27*, 435.
(28) Beurskens, P. T.; Admiraal, G.; Beurskens, G.; Bosman, W. P.; de Gelder, R.; Israel, R.; Smits, J. M. M. *The DIRDIF-94 Program System*; Technical report of the crystallography laboratory; Univeristy of Nijmegen; Nijmegen, The Netherlands, 1994.
(29) *teXsan*, A Crystal Structure Analysis Package; Molecular Structure Corporation: The Woodlands, TX, 1985 and 1992.
(30) (a) Becke, A. D. *J. Chem. Phys.* **1993**, *98*, 1372. (b) Becke, A. D. *J. Chem. Phys.* **1993**, *96*, 5648.

This method would give reliable geometries.[34] Normal coordinate analysis has been performed for all stationary points to characterize the transition states (TSs) and equilibrium structures. Therefore, the energy minimum structures reported in this paper show positive eigenvalues of the Hessian matrix, whereas TSs have one negative eigenvalue. For most TSs, the analysis including the visualization of the negative frequency was sufficient to specify the corresponding reaction path. In some cases, intrinsic reaction coordinate (IRC) calculations[35] near the TS region followed by geometry optimization of both reactants and products were performed to confirm the connectivity of the TSs. Unscaled vibrational frequencies were used to calculate zero-point energy (ZPE) corrections to total energy. The Gibbs free energies were also calculated employing the usual approximations of statistical thermodynamics (ideal gas, harmonic oscillator, and rigid rotor) at the temperature of 298.15 K and the pressure of 1.00 atm. Unless otherwise noted, the ZPE-corrected energies are used in the discussion.

Acknowledgment. Part of the calculations were carried out at the Research Center for Computational Science of Okazaki National Research Institutes, Japan. We acknowledge financial support (14654123 and 14044071) from Ministry of Education, Science, Sports, and Culture, Japan.

Supporting Information Available: X-ray crystallographic data (PDF) and optimized geometries of all the systems and their energy values. This material is available free of charge via the Internet at http://pubs.acs.org.

OM0208319

(31) Frisch, M. J.; Trucks, G. W.; Schlegel, H. B.; Scuseria, G. E.; Robb, M. A.; Cheeseman, J. R.; Zakrzewski, V. G.; Montgomery, J. A., Jr.; Stratmann, R. E.; Burant, J. C.; Dapprich, S.; Millam, J. M.; Daniels, A. D.; Kudin, K. N.; Strain, M. C.; Farkas, O.; Tomasi, J.; Barone, V.; Cossi, M.; Cammi, R.; Mennucci, B.; Pomelli, C.; Adamo, C.; Clifford, S.; Ochterski, J.; Petersson, G. A.; Ayala, P. Y.; Cui, Q.; Morokuma, K.; Malick, D. K.; Rabuck, A. D.; Raghavachari, K.; Foresman, J. B.; Cioslowski, J.; Ortiz, J. V.; Stefanov, B. B.; Liu, G.; Liashenko, A.; Piskorz, P.; Komaromi, I.; Gomperts, R.; Martin, R. L.; Fox, D. J.; Keith, T.; Al-Laham, M. A.; Peng, C. Y.; Nanayakkara, A.; Gonzalez, C.; Challacombe, M.; Gill, P. M. W.; Johnson, B.; Chen, W.; Wong, M. W.; Andres, J. L.; Gonzalez, C.; Head-Gordon, M.; Replogle, E. S.; Pople, J. A. *Gaussian 98, Revision A.11*; Gaussian, Inc.: Pittsburgh, PA, 1998.

(32) Hay, P. J.; Wadt, W. R. *J. Chem. Phys.* **1985**, *82*, 299.

(33) Hehre, W. J.; Ditchfield, R.; Pople, J. A. *J. Chem. Phys.* **1972**, *56*, 2257. (b) Hariharan, P. C.; Pople, J. A. *Theor. Chim. Acta* **1973**, *28*, 213. (c) Francl, M. M.; Pietro, W. J.; Hehre, W. J.; Binkley, J. S.; DeFrees, D. J.; Pople, J. A.; Gordon, M. S. *J. Chem. Phys.* **1982**, *77*, 3654.

(34) Foresman, J. B.; Frisch, A. E. *Exploring Chemistry with Electronic Structure Methods*, 2nd ed.; Gaussian Inc.: Pittsburgh, PA, 1995; Chapter 7, p 158.

(35) (a) Fukui, K. *Acc. Chem. Res.* **1981**, *14*, 363. (b) González, C.; Schlegel, H. B. *J. Chem. Phys.* **1991**, *95*, 5853.